

Fermilab

TM-964
2257.000

THOMAS R. CARDELLO

YALE UNIVERSITY

Design For a Short Charged Secondary Beam

September 1984

A primary beam target and dump along with a charged particle momentum defining channel was designed to provide a secondary beam 0.9cm high by 0.37cm wide with a momentum spread of 3.6% (σ) and angular divergence less than 1 milliradian.

Overview

This paper describes the design considerations for a short, high energy charged secondary beam. The goal was to produce a spacially small and well collimated beam with low momentum spread. Since we wished to study secondary particles with characteristic lifetimes between 2 and 5 cm, and with energies from 100 to 350 GeV, it was also necessary to completely define the beam within a short distance from their production site.

The following section states our design constraints. The remaining sections describe the principle beam defining systems.

Design Constraints

We require a compact charged particle beam of greater than 10^6 particles per pulse, with spotsize $.5 \text{ cm}^2$, small angular divergence (less than 1 mrad) and good momentum definition (15%). In order to produce this beam, we target up to 10^{12} protons at 400 GeV on one interaction length of copper. Immediately after the target is a 1.5 meter long beam dump designed to absorb the not interacting protons.

The target and the dump are placed inside the 400 ton hyperon magnet shown in figures 1a-b. This magnet was designed to provide a maximum field of 35 kgauss throughout its $7.7 \times 2.3 \times 731 \text{ cm}^3$ gap. A 5 meter long channel, which defines the secondary beam, was placed immediately after the dump inside the magnet. Figure 2 shows a schematic of the channel in the magnet. The particle composition of the resulting beam is described in Reference 1.

The nominal bend angle of the channel was chosen to be 21 mrad so that the maximum momentum of the transported beam would be 366 GeV. This precludes the possibility of transporting the high intensity 400 GeV primary beam through our apparatus.

In addition to the requirements of particle flux, beam size and momentum definition, the main considerations in the beam design were:

1. Matching the channel emittance to the acceptance of the downstream apparatus. An angular divergence less than 1 mrad and a momentum spread of less than 8 % RMS were required.
2. Ability to extrapolate particle tracks from the

channel exit back to the target. In order to utilize the position and angle correlation of a particle's track at the channel exit in determining its momentum, we must minimize the number of particles which scatter from the channel walls and exit with the beam.

3. Background reduction. Primaries that do not interact should be absorbed so as to minimize background due to their interaction products. Target produced, off-acceptance secondaries should be interacted in the dump before they can decay into muons.
4. Thermal integrity of the dump. Thermal stress in the dump must not affect the channel optics.

It is convenient to divide our system into three regions. Their locations and functions are described below. Note that we define our coordinate system as follows. The z axis lies along the principal centroid of the channel (central ray) and has constant curvature throughout the magnet. The Y axis points up and has its origin at the z axis. The x axis is defined to complete a standard right handed coordinate system. We also use an X1

axis which has its origin along the magnet center line and is perpendicular to both the Y axis and the magnet centerline. All lengths are in centimeters.

Target Region ($0.0 < Z < 45.7$)

The Target Region is shown in Figure 3A. The downstream z bound of this region is chosen so as to allow targets of up to 45 cm in length. The target (Figure 3B) is mounted on a manipulator which can place the target either in or out of the primary beam under remote control. Changing targets is done manually with minimal effort. The primary beam enters this region at $(X_1, Y, Z) = (-1.28, 0, 0)$. The central ray makes a 9.42 mrad angle with the magnet centerline at $Z=0$. The primary beam initially lies along the central ray when we wish to accept zero production angle secondaries. The primary beam targeting angle is variable by ± 7 mrad. When focused at the target, the primary beam is such that 95% (65%) of the beam hits a square spot of side 0.5mm (0.25mm).¹⁾

We initially chose a copper target with one interaction length (9 cm) and having square cross-section of width 0.10 cm. This width induces an uncertainty of 0.6% in a determination of a secondary particle's momentum when calculated from the exit position and angle of the

particle (see Appendix A). Secondary particle yields are estimated in Reference 1. Details of the target manipulator and targets can be found in the Fermilab Proton Department drawings listed at the end of this paper.

To allow for target monitoring, three 1.27 cm diameter holes were drilled into the upper pole piece of the magnet at $(Z, X_1) = (19.60, +0.79)$; $(19.606, -0.71)$; $(19.606, -2.77)$ (see Figure 4). A 7.62 cm wide by 2.54 cm deep slot was centered onto the downstream face of the first upper magnet lamination in order to provide a vertical flight path from the target monitoring holes to the top of the magnet. Scintillators are placed above the slot to provide for target monitoring.

Dump Region ($45.7 < Z < 198$)

Figure 5 shows the dump area in relation to the target. The choice of the downstream z bound of this region is described in section 1.4. The dump walls are sloped so that particles from the target which intercept the dump will have their reaction products remain in the dump as long as those products have P_t / P less than 0.013²⁾ This is illustrated in Figure 6A. Figure 6B gives examples where the primary beam hits the dump.

In order to absorb particles incident on the dump we desire a material with a short absorption length. We chose a tungsten alloy ³⁾ because of its 10 cm absorption length, high thermal conductivity, high strength and ease in machining.

The thermal impact of the beam on the dump is shown in Figure 7, where ΔT is the temperature rise of the dump at R_0 , the radial distance from the primary beam axis. The energy deposition profile of the beam was determined using the CASM program by A. Van Ginnekin of Fermilab.

The dump is water cooled by two closed-loop, .62 CM diameter copper tubes (see Figure 5). Thermocouples are placed in the dump at $Z = 91$ cm and $Z = 182$ cm. The energy deposition in the dump at 10^{12} protons per pulse is 64 KJoules per pulse. If we are conservative and assume that all the deposited heat must be carried away by the coolant, we require a flow of at least 0.15 liters per second through the loops in order to keep the temperature rise in the coolant less than 10° C.

Channel Region (198. < Z < 731.4)

Both the horizontal and vertical projections of the channel along the channel centroid form sections of cones (see

Figure 8). The target lies inside the cones and as close as possible to their common apex at $Z = -100$ cm. The channel cross-section is rectangular. For such a channel, the horizontal and vertical half widths (X_E, Y_E) of the channel at its downstream end, and the radius of curvature (ρ) of the channel centroid fix the channel design. The following scaling arguments illustrate how the channel parameters are selected to achieve a desired particle flux and momentum acceptance.

In order to determine X_E, Y_E and ρ , we consider first a channel of square cross-section, so $X_E = Y_E = S$. Let $\Delta P/P$ be the momentum spread of the beam exiting the channel. Let $\Delta\Omega$ be the solid angle subtended by the channel exit aperture as seen from the target. The particle flux requirements constrain $\Delta\Omega \cdot \Delta P/P$, and since:

$$\Delta\Omega \cdot \Delta P/P \sim \rho X_E^2 Y_E = \rho S^3 = \text{constant},$$

we thus have S as a function of ρ .

We also wish to keep the particle flux constant when we vary X_E and Y_E at constant ρ . This allows a parametrization of X_E and Y_E in terms of the aspect ratio R defined via:

$$Y_E = RS \text{ and } X_E = S/\sqrt{R}$$

Variation of R leaves $\rho X_E^2 Y_E$ and hence the exiting particle flux invariant.

So the question of picking ρ , X_E and Y_E boils down to picking ρ and R. Note that the nominal $\Delta P/P$ is determined once one chooses ρ and R, so by examining our $\Delta P/P$ requirements, and the constraints on the exiting beam's position and angle space imposed by the apparatus downstream of the channel, we arrive at some ρ and R. The desire to transport 350 GeV particles through a 35 KG field determines a nominal ρ we call ρ_0 . Figure 9 plots ρ/ρ_0 versus R for a few $(\Delta P/P)_{\max}$. The constraints from the downstream apparatus are also shown. We chose the channel with $(p, X_E, Y_E) = (34831, .186, .45)$ corresponding to an R of 1.8 and a $(\Delta P/P)_{\max} \approx .07$. The solid angle subtended by the channel exit for central momentum particles originating at the target is 0.62 μ sterad.

After the shape of the channel was chosen the z coordinates of the transitions between the dump and channel were determined. In the vertical plane the transition occurs at $Z = 274$ cm, and in the horizontal at $Z = 198$ cm. The horizontal transition point was a compromise between refining $\Delta P/P$ ⁴⁾, which favors small Z, and the need for a

reasonable range of forbidden horizontal targeting angles. A forbidden targeting angle is an angle at which a substantial fraction of the not interacting primary beam particles hit the upstream aperture of the channel. We chose $Z = 198$ cm. The desire to resolve target produced secondaries from backgrounds and to limit the range of forbidden vertical targeting angles indicated a large Z vertical transition. $Z = 274.3$ cm is the longest vertical transition which allows adequate cooling of the dump since it was practical to extend the cooling loop only through $Z = 335.3$ cm. Using the vertical position and angle information on a particle's track from our downstream apparatus, we can resolve greater than 80% of the channel area at $Z = 274.3$ cm. Figure 10 shows the forbidden region of horizontal targeting angle versus central ray momentum.

The beam exiting the channel can be divided into clean and scattered components. The clean component exits the channel without interacting (after the target), whereas the scattered component interacts in the channel walls. The scattered component was modeled by a Monte Carlo Program described in Appendix B, and was determined to comprise $\approx 10\%$ of the beam exiting our final channel. The Monte Carlo was also useful as a check on our analytically calculated channel parameters, e.g. the RMS deviation of $\Delta P/P$ obtained from the Monte Carlo was 3.6%. Inelastic

interactions were not modeled. Figures 11 show some phase space plots of the beam at the channel exit. We note that the muon to pion ratio at the channel exit is 0.06 ± 0.002 for 10^6 pions exiting the channel and for muons within a $3 \times 3 \text{ cm}^2$ area centered at $x = y = 0$. (see Reference 4)

Bells and Whistles

Helium feed tubes were placed at either end of the magnet inner tunnels in order to fill the channel with helium and thus minimize multiple scattering. There is also a gas barrier at $Z = 655 \text{ cm}$ and the channel walls are aluminized between $Z = 655 \text{ cm}$ and $Z = 731 \text{ cm}$. This forms part of a light particle tagging Cerenkov counter (see Reference 2). A Hall probe is located at $(X, Y, Z) = (3.4, 0., 714.)$.

- 1) The previous occupants of Fermilab P-center, E288, could place 95%(85%) of the primary beam on a square spot of side 0.04cm(0.02cm).* Our target is 36m(versus 27m for E288) from the center of the P-center quadropole string. At the above percentages we thus expect a spotsize of $4/3(0.04)$ cm and $4/3(0.02)$ cm respectively.

*A. Ito, private communication

- 2) This is true for single scattering. For plural scattering, $P_{i\perp}$ and P_i be the particle's transverse momentum and momentum at the i^{th} scatter. For $P_{i\perp} \ll P_i$ we require $\sum_i \frac{P_{i\perp}}{P_i} \leq 0.013$ for the particle to remain in the dump.

- 3) Teledyne powder alloys metal densalloy 18, an alloy of copper and tungsten with density 18g/cc. Referred to as "Hevimet".

- 4) For a point target, variation of the horizontal transition point has no effect. Since the target has a finite length and width, horizontal transition point variation refines the $\left. \frac{\Delta P}{P} \right|_{\text{MAX}} \sim 7\%$ arrived at in fixing (ρ, X_E, Y_E) .

- Reference 1 Fermilab TM 818 2060.000, K. Doroba
Hyperon and Antihyperon fluxes in the Fermilab
Charged Hyperon Beam.
- Reference 2 To be published, T. Cardello
A Light Particle Threshold Čerenkov Counter.
- Reference 3 Phys. Rev. D. 1 Nov 78, p.3115, vol. 18
P. Skubic, et al.
- Reference 4 E497 Note, K. Doroba
"Halo" program calculation of muon background.
- Reference 5 Ph.D. thesis, Yale University, 1979, Alan Schiz
and private communication.
- Reference 6 UCRL Range Tables, Σ^+ in Pb.
- Reference 7 B. Rossi, High Energy Particles, Prentice-Hall,
New York, QC721.R735

Appendix A

We define the following:

- X_0 = production position of particle
 X_1 = position of particle at 1st PWC
 X_2 = position of particle at 2nd PWC
 θ_0 = production angle of particle
 θ_{MSi} = angle change due to multiple scattering of particle in Region i
 X_{MSi} = position change due to multiple scattering of particle in Region i
 ρ_0 = radius of curvature of channel's central ray
 L_{Ri} = radiation length of material i
 $\frac{\Delta P}{P} = \left(\frac{P - P_{CR}}{P} \right)$; P = particle's momentum
 P_{CR} = central ray momentum

Figure A-1 is a schematic of a particle track from the target to the 2nd PWC station. We calculate the error in an estimate of the particle's $\frac{\Delta P}{P}$ when calculated from the particle's position at the two PWC stations.

We calculate $\frac{\Delta P}{P}$ as a function of X_0 , X_1 and X_2 :

$$\begin{aligned}
 X_1 &= X_0 + \frac{\Delta P}{P} \frac{\hat{L}^2}{2\rho_0} + \theta_0 L \\
 \theta_1 &= \theta_0 + \frac{\Delta P}{P} \frac{\hat{L}}{\rho_0} \\
 X_2 &= X_0 + \frac{\Delta P}{P} \frac{\hat{L}^2}{2\rho_0} + L\theta_1 - \frac{L\hat{L}}{\rho_0} \frac{\Delta P}{P} \\
 &= X_0 + L\theta_1 + \frac{\Delta P}{P} \alpha \quad ; \quad \alpha = \left[\frac{\hat{L}^2}{2\rho_0} - \frac{L\hat{L}}{\rho_0} \right]^{-1} = -0.117
 \end{aligned}$$

$$\frac{\Delta P}{P} = \alpha (X_o - X_1 + L \theta_1) ; \quad \theta_1 = \frac{X_2 - X_1}{L_4}$$

$$\frac{\Delta P}{P} = \alpha \left[X_o - X_1 \left(1 + \frac{L}{L_4}\right) + \frac{L}{L_4} X_2 \right]$$

$$\partial_{X_o} \left(\frac{\Delta P}{P} \right) = \alpha = -0.117$$

$$\partial_{X_1} \left(\frac{\Delta P}{P} \right) = -\alpha \left(1 + \frac{L}{L_4}\right) = 0.721$$

...eqs 1

$$\partial_{X_2} \left(\frac{\Delta P}{P} \right) = \alpha \frac{L}{L_4} = -0.604$$

Now we calculate the error matrix for the variables X_o , X_1 , and X_2 .

Consider \tilde{X}_i to be the measured value of X_i

$$\tilde{X}_1 = X_1 + X_{PW1} + X_{MS13}$$

$$\tilde{X}_2 = X_2 + X_{PW2} + X_{MS14}$$

We have defined X_{PW_i} to be the resolution of PWCi and X_{MSij} to be the multiple scattering error in traveling through regions $i, i+1, \dots, j$.

We have, redefining $X_1 \rightarrow \tilde{X}_1 - X_1$

$$\langle X_1^2 \rangle = \langle X_{PW1}^2 \rangle + \langle X_{MS13}^2 \rangle$$

$$\langle X_2^2 \rangle = \langle X_{PW2}^2 \rangle + \langle X_{MS14}^2 \rangle$$

$$\langle X_1 X_2 \rangle = \langle X_{MS13} X_{MS14}^2 \rangle$$

Now

$$X_{MS14} = X_{MS13} + L_4 \theta_{MS13} + X_{MS4}$$

So equations 2 become

$$\begin{aligned} \langle X_1^2 \rangle &= \langle X_{PW1}^2 \rangle + \langle X_{MS13}^2 \rangle \\ \langle X_2^2 \rangle &= \langle X_{PW2}^2 \rangle + \langle X_{MS13}^2 \rangle + L_4^2 \langle \Theta_{MS13}^2 \rangle + \langle X_{MS4}^2 \rangle \\ &\quad + 2L_4 \langle X_{MS13}^\Theta \rangle \\ \langle X_1 X_2 \rangle &= \langle X_{MS13}^2 \rangle + L_4 \langle X_{MS13}^\Theta \rangle \end{aligned}$$

Defining $\beta = \left(\frac{0.011}{F}\right)^2$, we have

$$\begin{aligned} \langle X_{MS13}^2 \rangle &= 1/3 L_i^2 \langle \Theta_{MS1i}^2 \rangle \Big|_{i=1,3} \\ &= 1/3 \beta \frac{L_i^3}{L_{Ri}} \Big|_{i=1,3} \\ \langle X_{MS4}^2 \rangle &= 1/3 \beta L_4^2 \left[\frac{L_4}{L_{R4}} + 0.011^* \right] \\ \langle \Theta_{MS13}^2 \rangle &= \beta \frac{L_i}{R_i} \Big|_{i=1,3} \\ \langle X_{MS13}^\Theta \rangle &= 1/2 \beta \frac{L_i^2}{L_{Ri}} \Big|_{i=1,3} \end{aligned}$$

Using the above, equations 2 become

$$\begin{aligned} \langle X_1^2 \rangle &= \langle X_{PW1}^2 \rangle + 1/3 \beta \frac{L_i^3}{L_{Ri}} \Big|_{i=1,3} \\ \langle X_2^2 \rangle &= \langle X_{PW2}^2 \rangle + 1/3 \beta \frac{L_i^3}{L_{Ri}} + \beta L_4^2 \frac{L_i}{L_{Ri}} + 1/3 \beta L_4^2 \left[\frac{L_4}{L_{R4}} + 0.011^* \right] \\ &\quad + \beta L_4 \frac{L_i^2}{L_{Ri}} \Big|_{i=1,3} \\ \langle X_1 X_2 \rangle &= 1/3 \beta \frac{L_i^3}{L_{Ri}} + 1/2 \beta L_4 \frac{L_i^2}{L_{Ri}} \Big|_{i=1,3} \end{aligned}$$

*0.011 compensates for multiple scattering in first PWC.

See E69 Note, DR30, L.Fajardo.

Using $P = 100\text{GEV}$

$$L_{R1} = 5.3\text{E-}5\text{cm}$$

$$L_{R2} = 4.0\text{E-}3\text{cm}$$

$$L_{R3} = L_{R4} = 3.0\text{E-}4\text{cm}$$

We have, with $\langle X_{PW1}^2 \rangle = \langle X_{PW2}^2 \rangle = 4.9\text{E-}5\text{cm}^2$

$$\langle X_0^2 \rangle = (\text{target } \frac{1}{2}\text{width})^2 = 2.5\text{E-}3\text{cm}^2$$

$$\langle X_1^2 \rangle = 5.380\text{E-}5\text{cm}^2$$

$$\langle X_2^2 \rangle = 7.496\text{E-}5\text{cm}^2 \quad \dots\text{eqs } 2$$

$$\langle X_1 X_2 \rangle = 8.635\text{E-}6\text{cm}^2$$

Using equations 1 and 2, and evaluating $\partial(E)\partial^T$, we have

$$\begin{aligned} \left(\partial \frac{\Delta P}{P}\right)^2 &= \left(\partial_{X_0} \frac{\Delta P}{P}\right)^2 \langle X_0^2 \rangle + \left(\partial_{X_1} \frac{\Delta P}{P}\right)^2 \langle X_1^2 \rangle + \left(\partial_{X_2} \frac{\Delta P}{P}\right)^2 \langle X_2^2 \rangle \\ &\quad + 2\left(\partial_{X_1} \frac{\Delta P}{P}\right)\left(\partial_{X_2} \frac{\Delta P}{P}\right) \langle X_1 X_2 \rangle \end{aligned}$$

$$\left(\partial \frac{\Delta P}{P}\right)^2 = 9.33\text{E-}5$$

$$\Rightarrow \partial \frac{\Delta P}{P} = 0.96\%$$

$\partial \frac{\Delta P}{P}$ due to target width alone is 0.6%

Appendix B

In the hyperon channel Monte Carlo, hyperons were produced at the target by an incident primary proton beam and then propagated in one step until they encountered a channel boundary. If a particle intersected the channel wall its path length before interaction was calculated and then it was propagated, taking $\frac{DE}{DX}$ and multiple scattering into account, until it either exited the magnet or interacted. This procedure continued until the particle was absorbed (or exited the magnet).

Three types of interactions were modeled. Coherent nuclear scattering, incoherent nuclear scattering and absorption. Parameters such as momentum and position were output immediately before and after each interaction.

The following relations were used:

Particle Production: (see Reference 3)

$$\frac{d\sigma}{d(P_{\perp}, X)} = e^{f(X, P_{\perp})} (1-X)^{g(P_{\perp})} ; \quad X = \text{Feynman } X$$

$$f = C_1 + C_2 X^2 + C_3 X + C_4 X P_T + C_5 P_T^2 + C_6 P_T^4 + C_7 P_T^6$$

$$g = C_8 + C_9 P_T^2$$

Quasi Elastic Scattering: (see Reference 5)

Let σ_{INT} be the interaction cross-section

$$\frac{\sigma_{QE}}{\sigma_{INT}} = 6.28 \text{ E-2}$$

$$\frac{d\sigma_{QE}}{db} \propto e^{bt}$$

Elastic Scattering: (see Reference 5)

$$\frac{\sigma_{EL}}{\sigma_{INT}} = 0.645$$

$$\frac{d\sigma_{EL}}{dq} \propto q \frac{J_1(2\sqrt{b_A} f)^2}{2\sqrt{b_A} f} \quad ; \quad J = \text{Bessel function}$$

$b_A = \text{forward coherent scattering slope}$

$q^2 = -t$

Absorption: (see Reference 6)

$$\frac{\sigma_{AB}}{\sigma_{INT}} = 0.292$$

$$\frac{DE}{DX} = \left(\frac{E}{100}\right)^{0.1046} \text{ (GEV/gm/cm}^2\text{)}$$

Multiple Scattering: (see Reference 7)

$$W(X, \eta) = \frac{\lambda\sqrt{3}}{2\pi T^2} e^{-\lambda/T(\eta^2 - 3\eta X/T + 3\frac{X^2}{T^2})}$$

$W(X, \eta)$ = probability density of scattering into X, η

X = displacement from unscattered path

η = Δ change in direction of \vec{P} with respect to unscattered path

T = distance traversed

$$\lambda = 2L_R \frac{P}{(0.015)^2} \quad ; \quad L_R = \text{radiation length}$$

The program simulated the production of hyperons from a beryllium target using the relation of Skubic, et al. The material modeled by the program for the channel walls was tungsten. Beam particles underwent no $\frac{DE}{DX}$ or multiple scattering while in the channel and the magnetic field was

assumed to be uniform and \perp to the plane of the channel centroid. If a particle was absorbed, no further tracking of the interaction products was done.

Fermilab Proton Department Drawings:

Target and Manipulator:

3497.133 - ME 76296
MB 76319 thru MB 76325
MC 76326
MC 76327
MD 76328
MC 76344
MB 76329 thru MB 76334
MD 76335
MB 76336 thru MB 76338
MD 76339
MC 76340
MB 76341
MB 23536
MB 42603
MB 76342
MB 76343

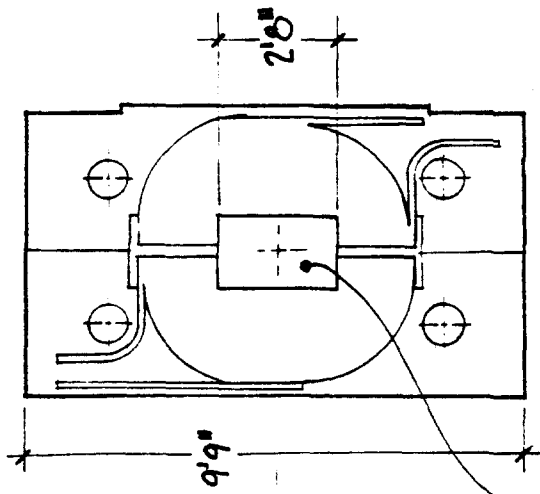
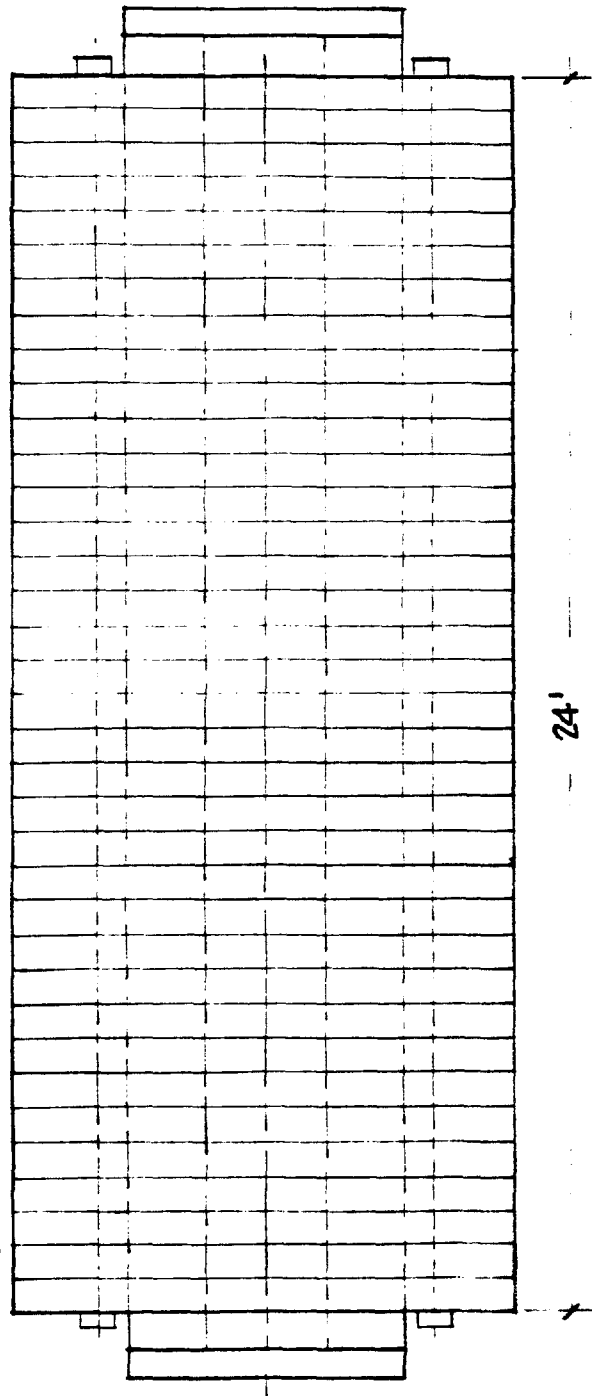
Dump and Channel Drawings:

master: 3497.133-LE 76205
3497.133-MC 76206 thru MC 76214
MC 76216 thru MC 76224

Inner and Outer Tunnels:

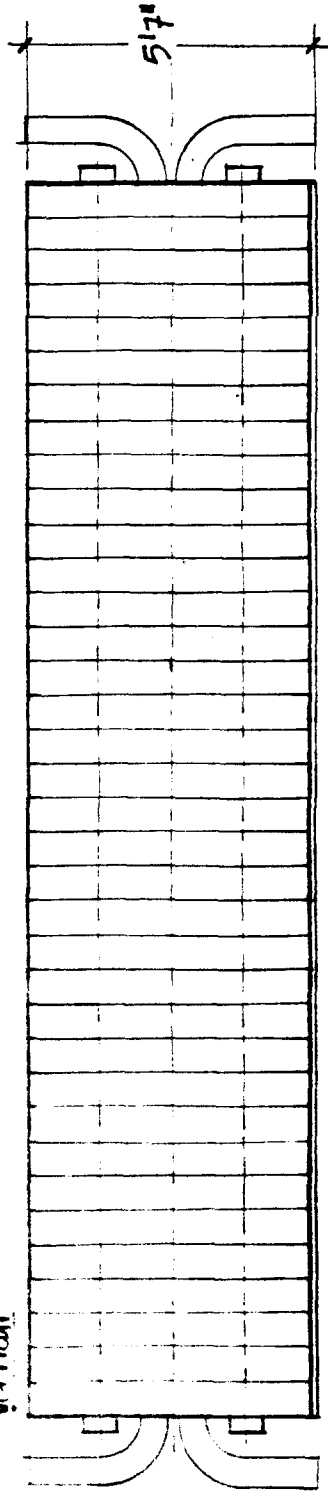
6023-ME 76150 thru ME 76153

horizontal



see Figure 1B for detail

vertical



HYPERON TARGET MAGNET

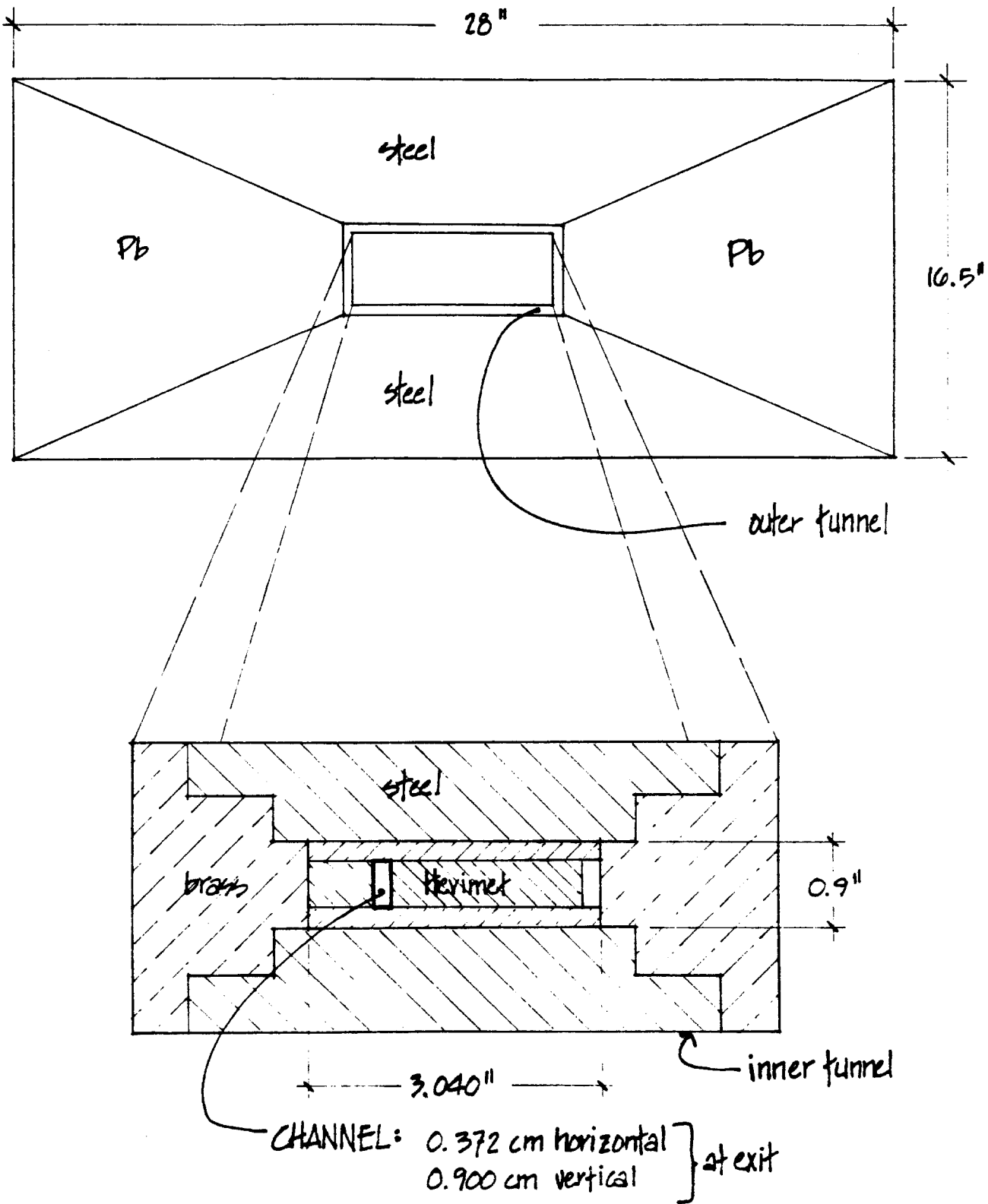
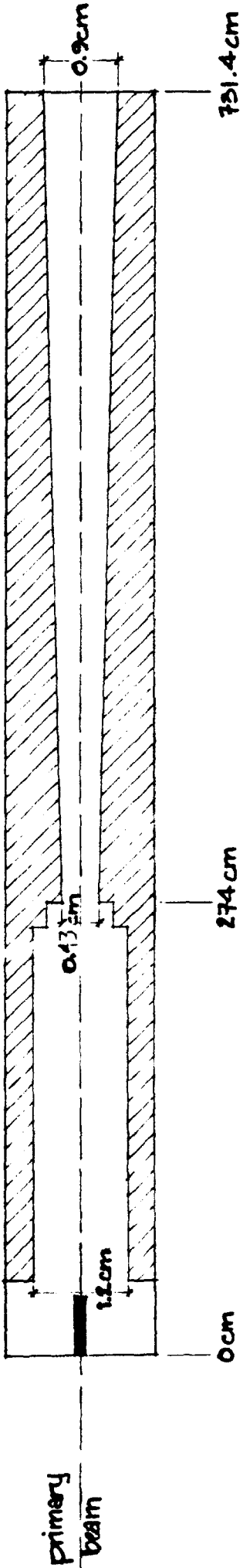


Figure 1-B

VERTICAL SECTION



HORIZONTAL SECTION

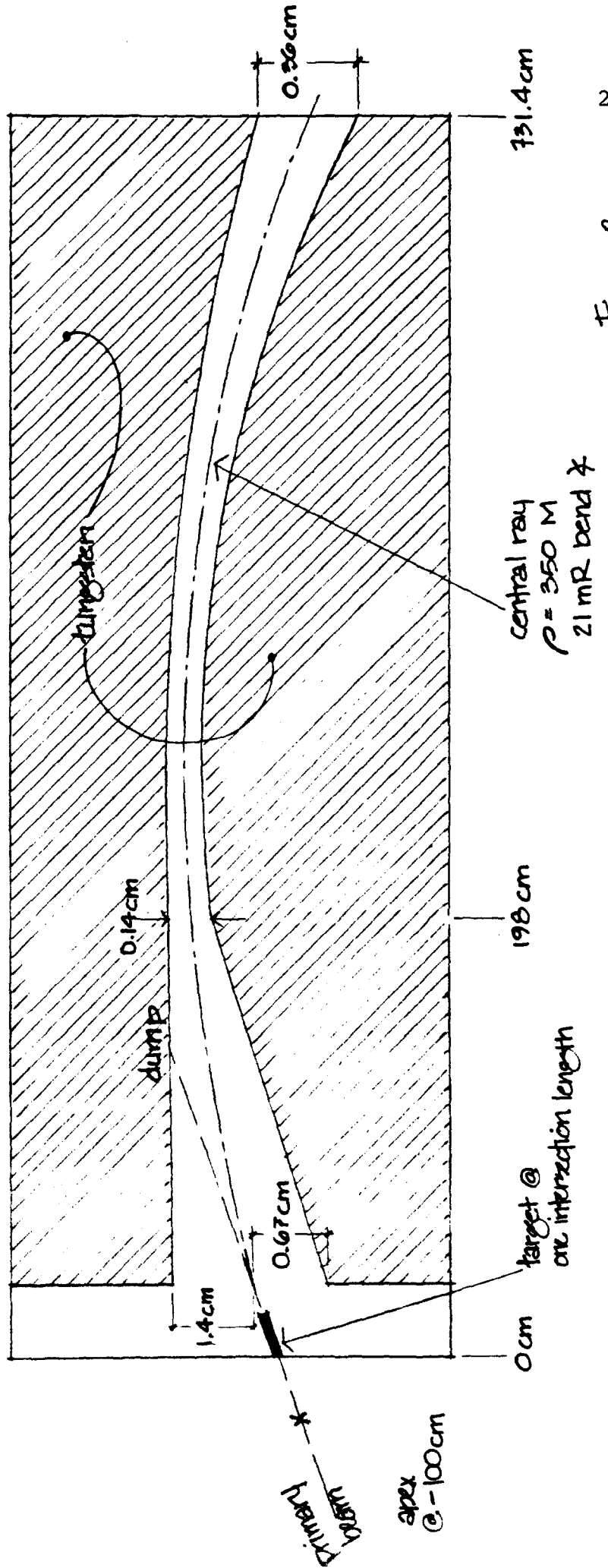


Figure 2

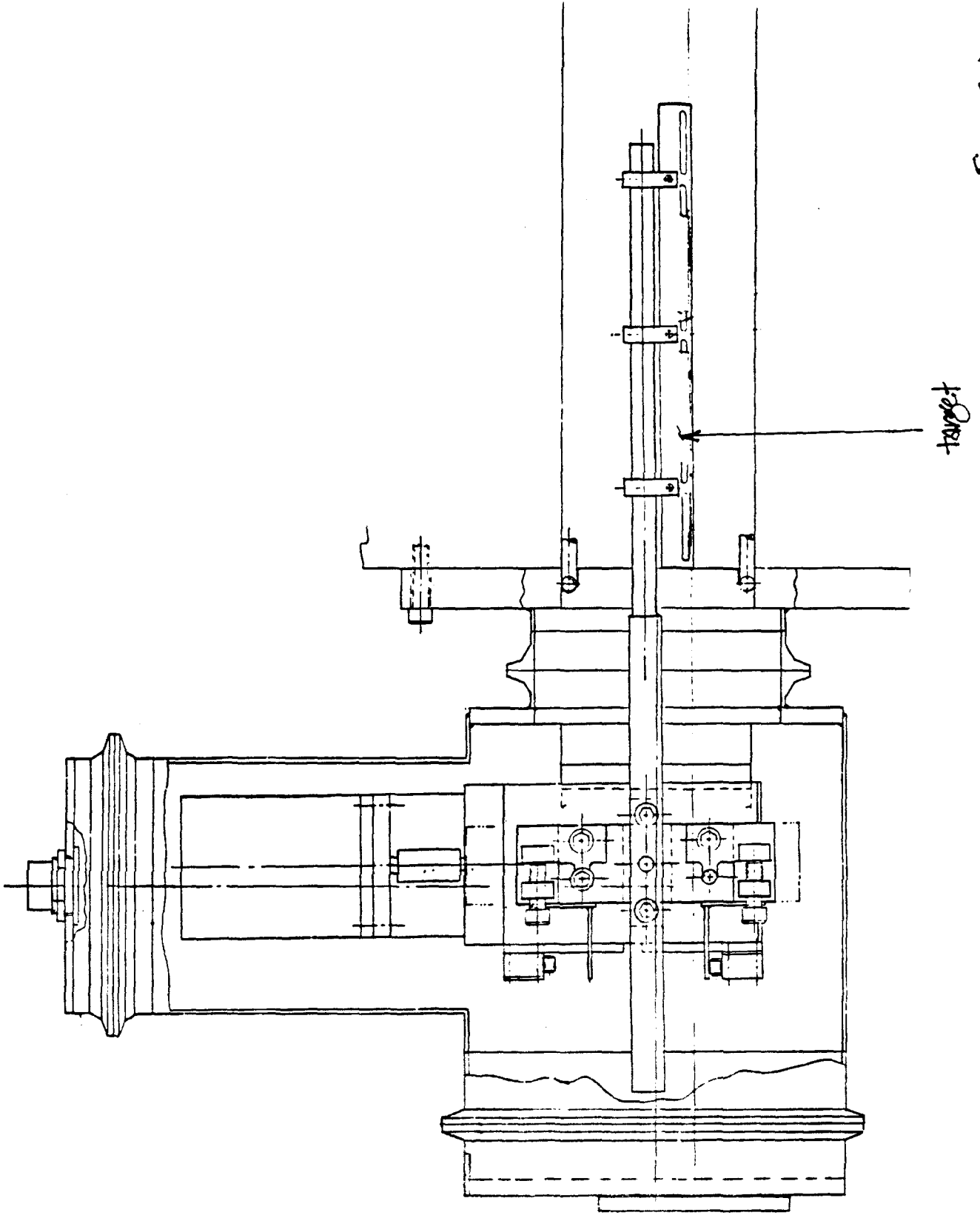
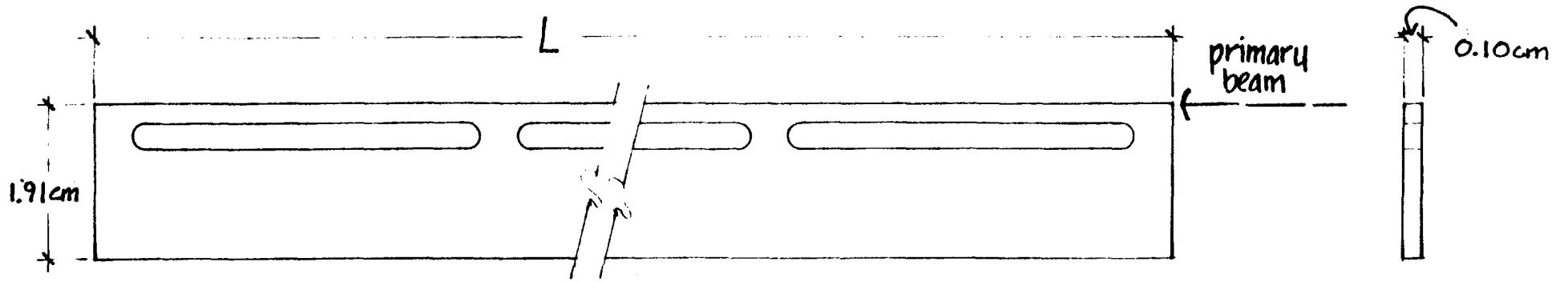
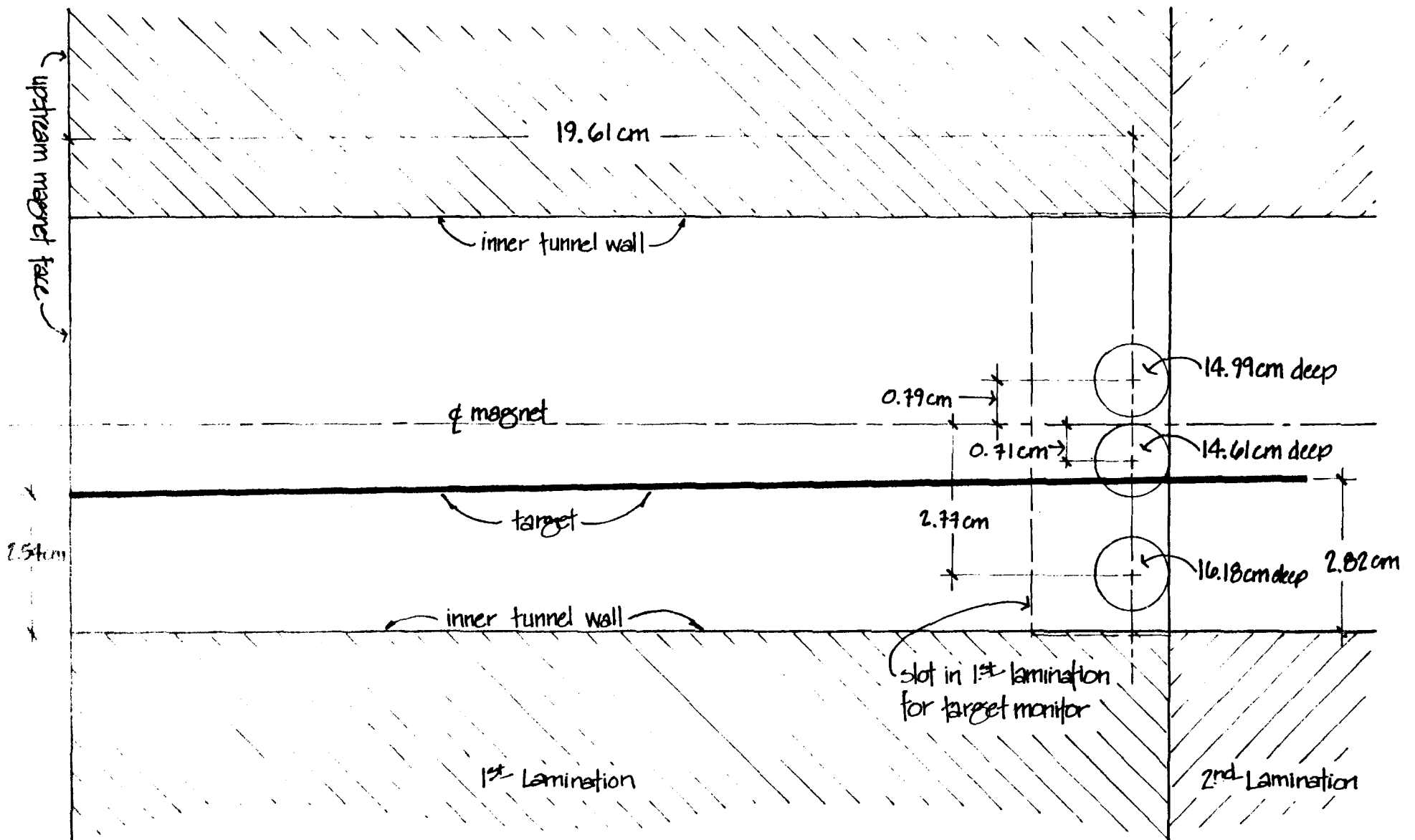


Figure 3.A



	beryllium	copper		aluminum
$L[\text{cm}]$	18.35	14.8	2.96	18.6

Figure 3B



30.48 cm long target shown, not to scale

Target positionings and target monitoring holes

Figure 4

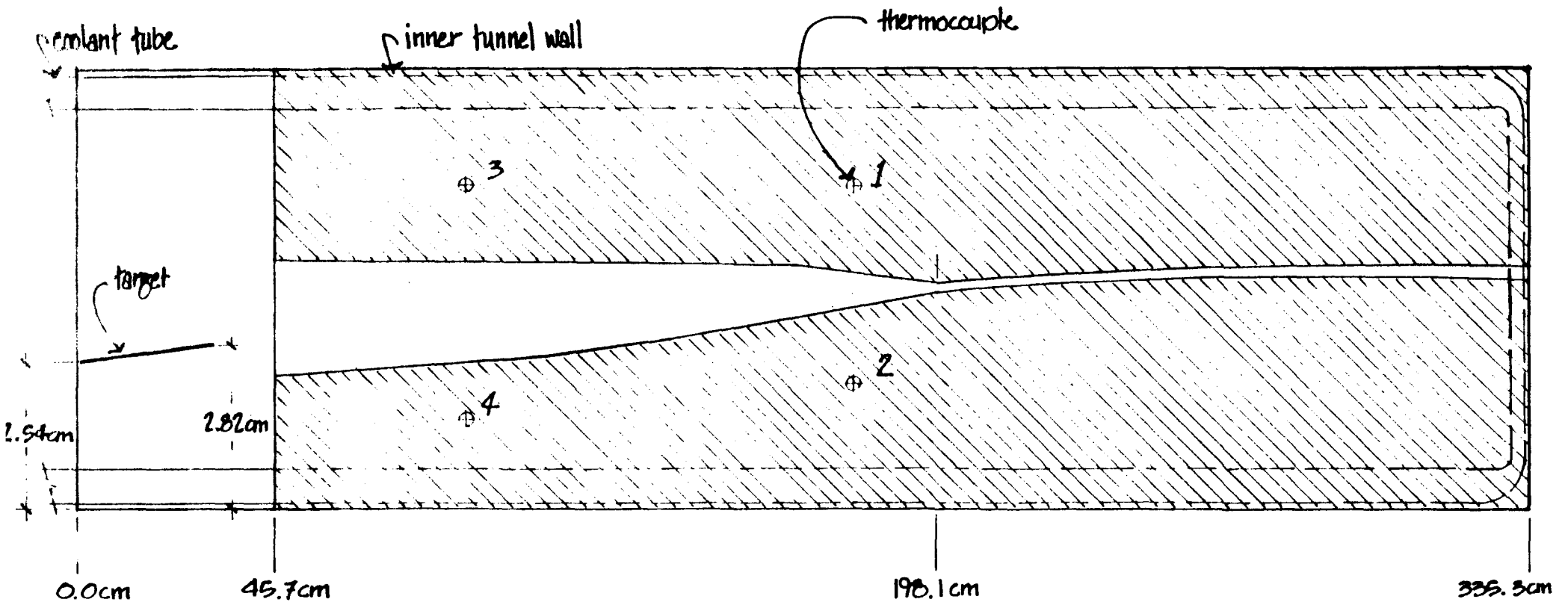
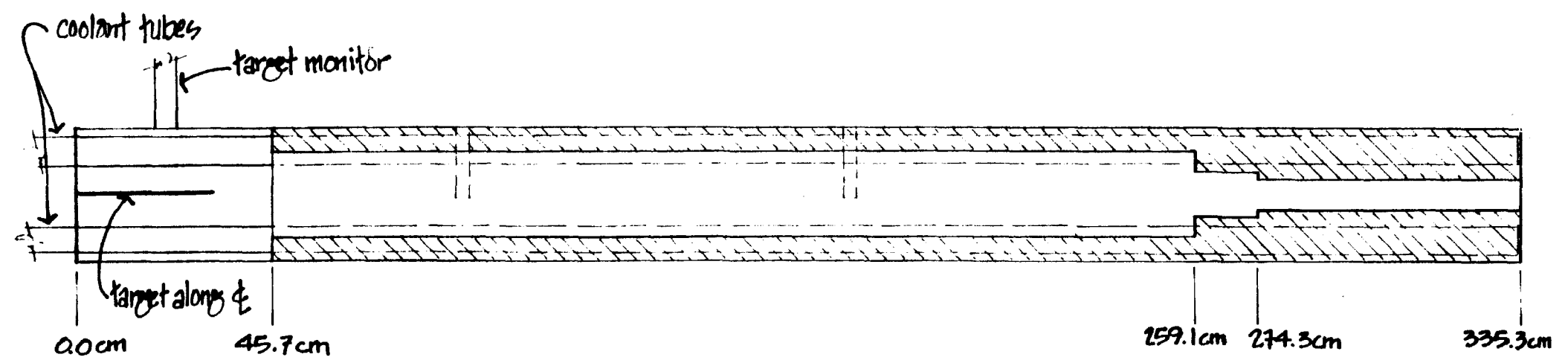
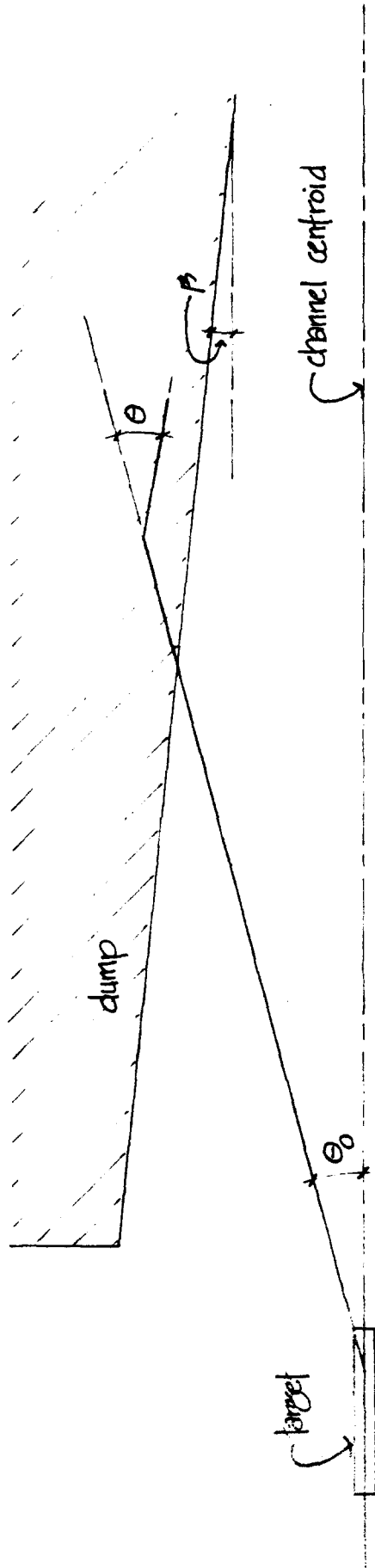
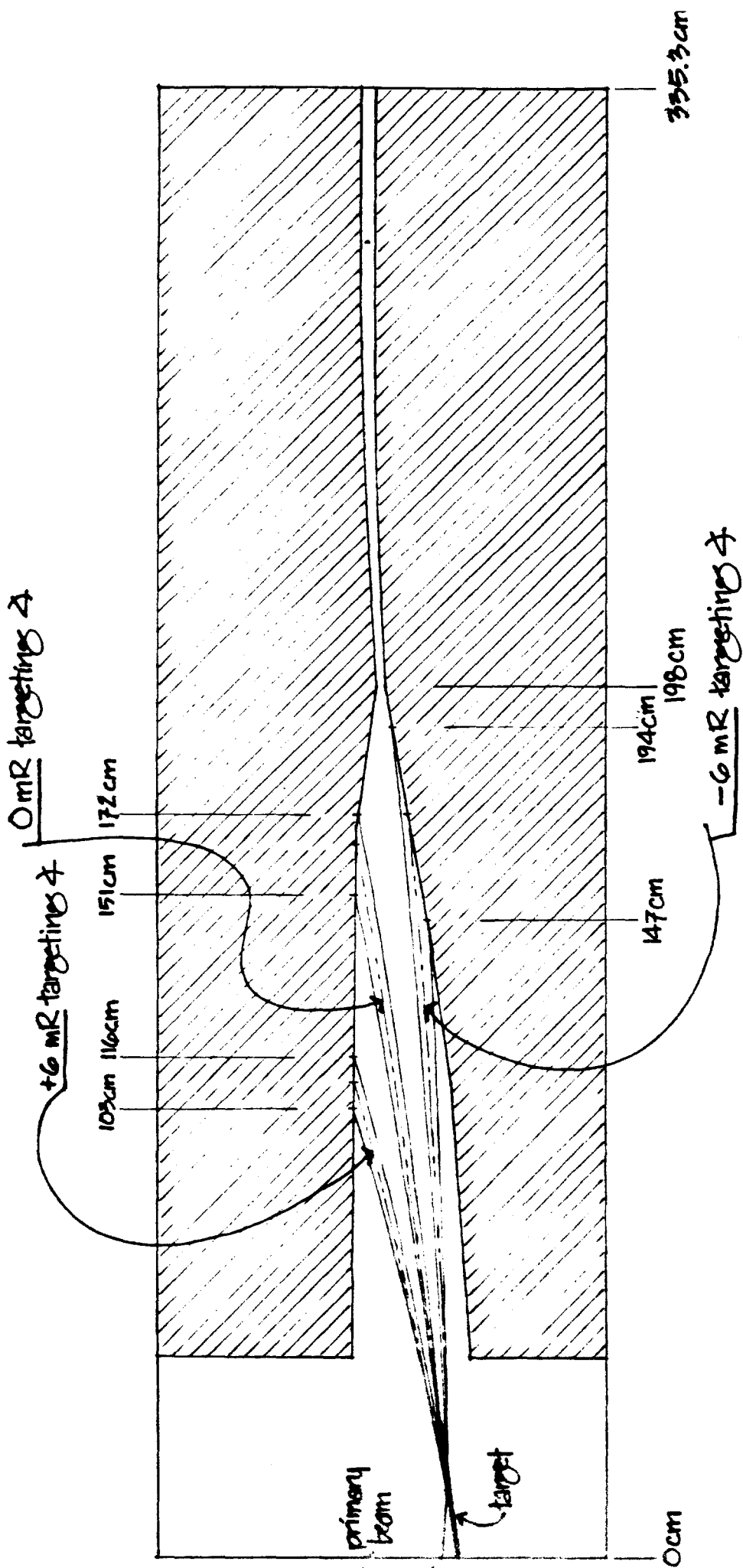


Figure 5



if $\theta_0 - \theta < \beta$, products of interactions in the dump do not exit the dump.
 For $P_L = 1.6\text{eV}$, $P = 75\text{ GeV}$ $\theta = 1/75$. If $\beta = 1/75$,
 these interaction products remain in the dump.

Figure 6.A



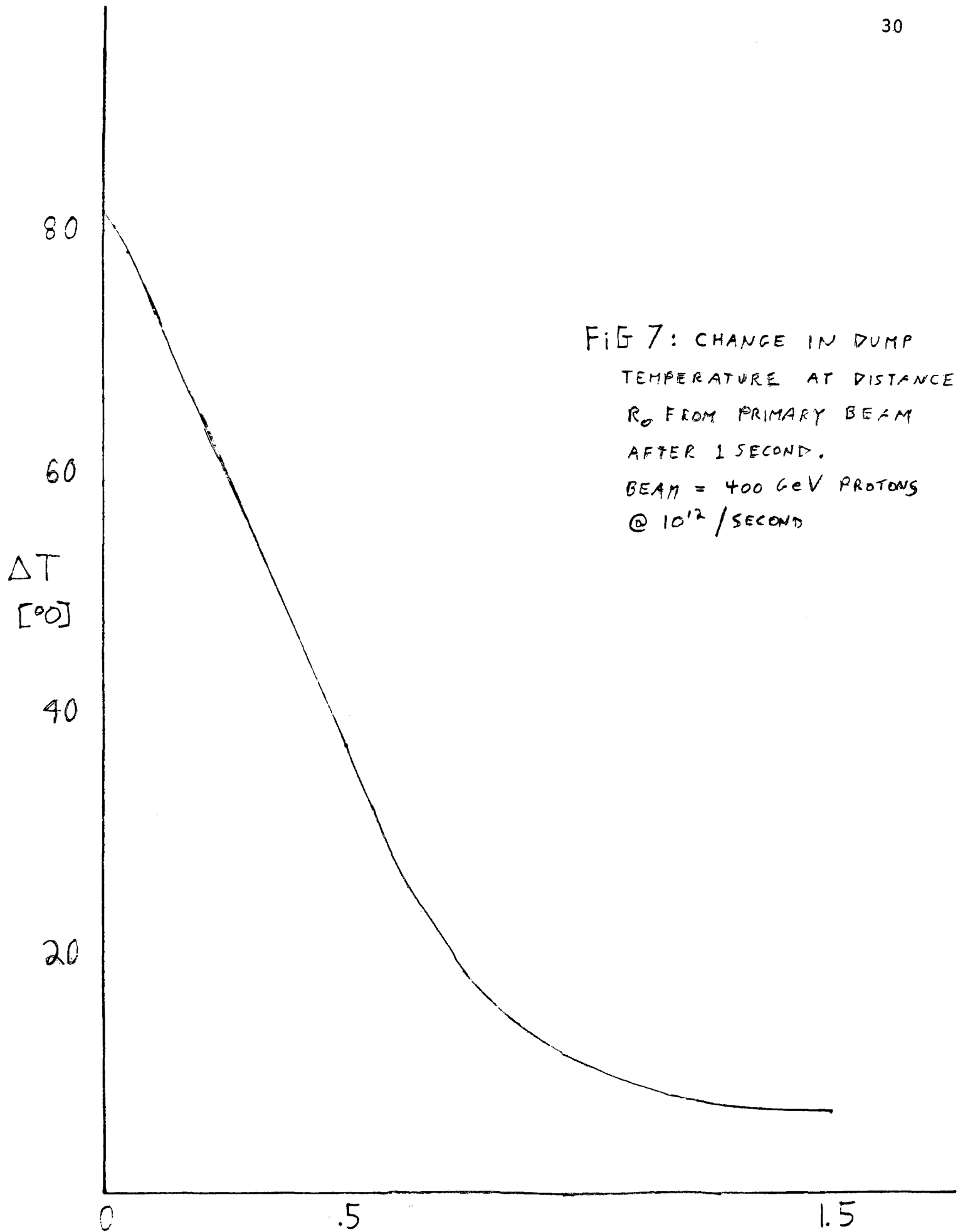
Primary Beam in the dump region

Primary = 400 GeV

Central ray = -250 GeV

primary beam divergence = ± 1 mR

Figure 6B



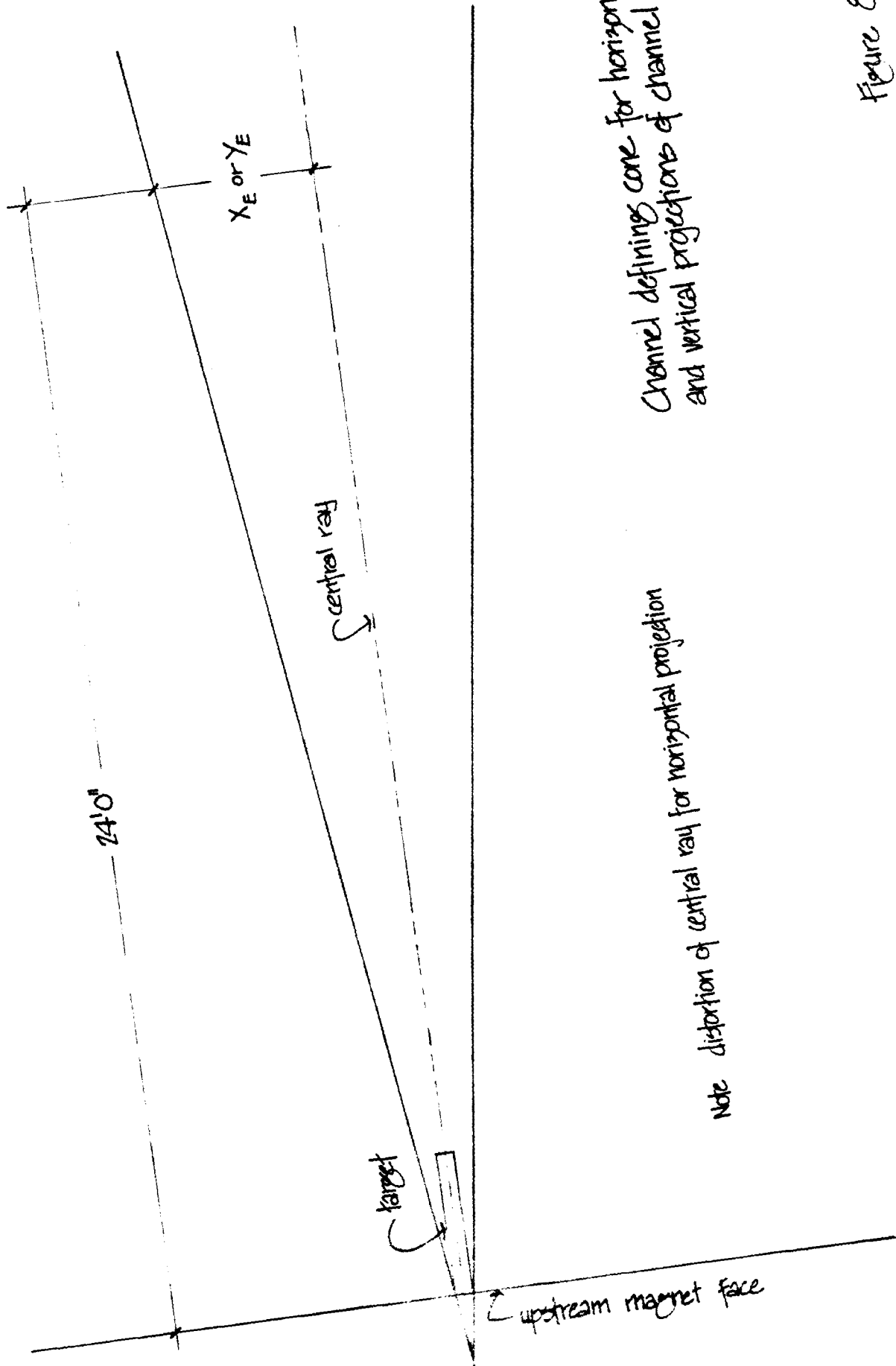


Figure 8

$$\frac{\Delta P}{P} \Delta \Omega = \pm 4.6\% \text{ } \mu\text{s}$$

$$S_p = f_0 = \pm 0.25 \text{ cm}$$

$$\delta = \left. \frac{\Delta P}{P} \right|_{\text{MAX}}$$

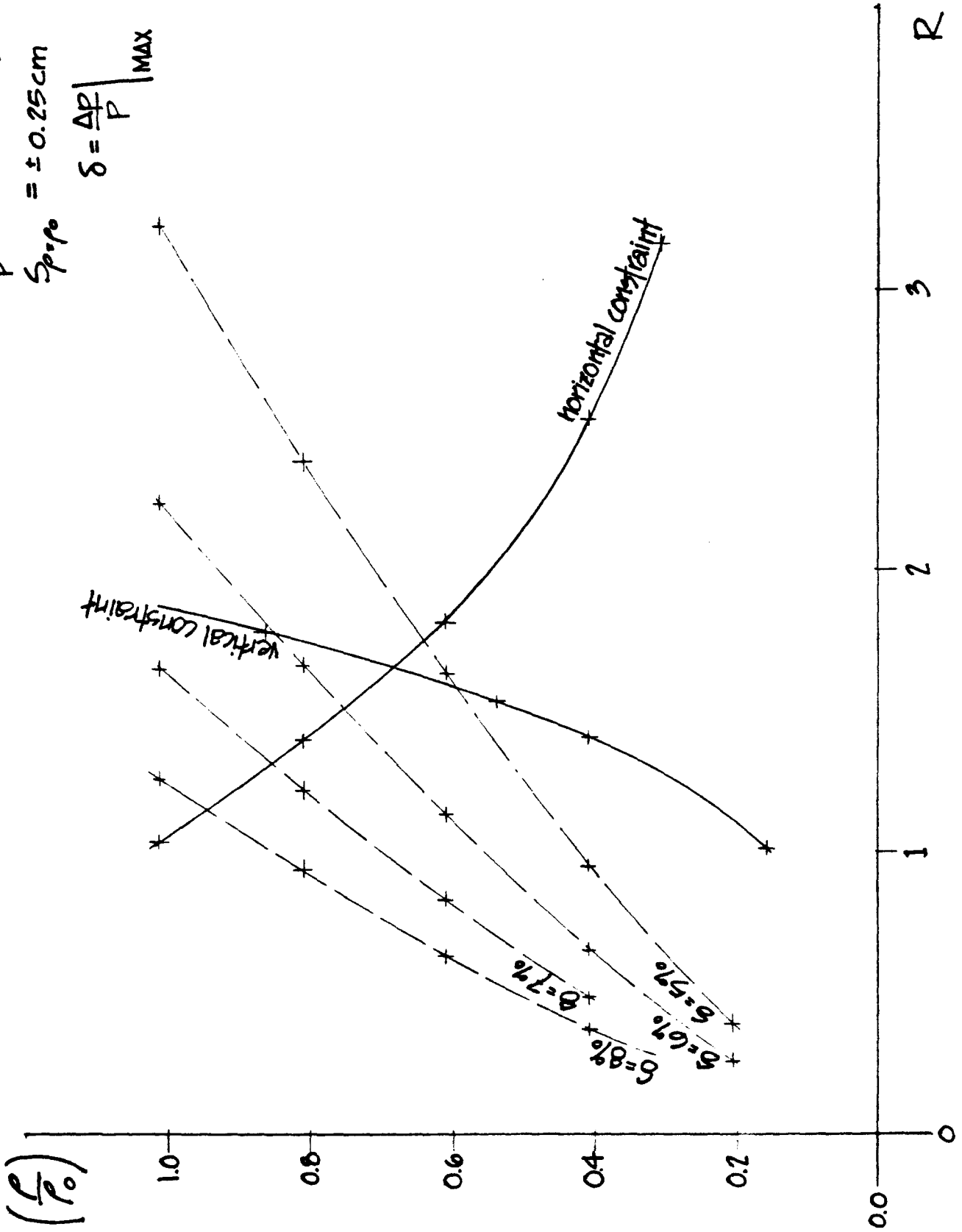


Figure 9

Forbidden targeting
angles versus central
ray momentum

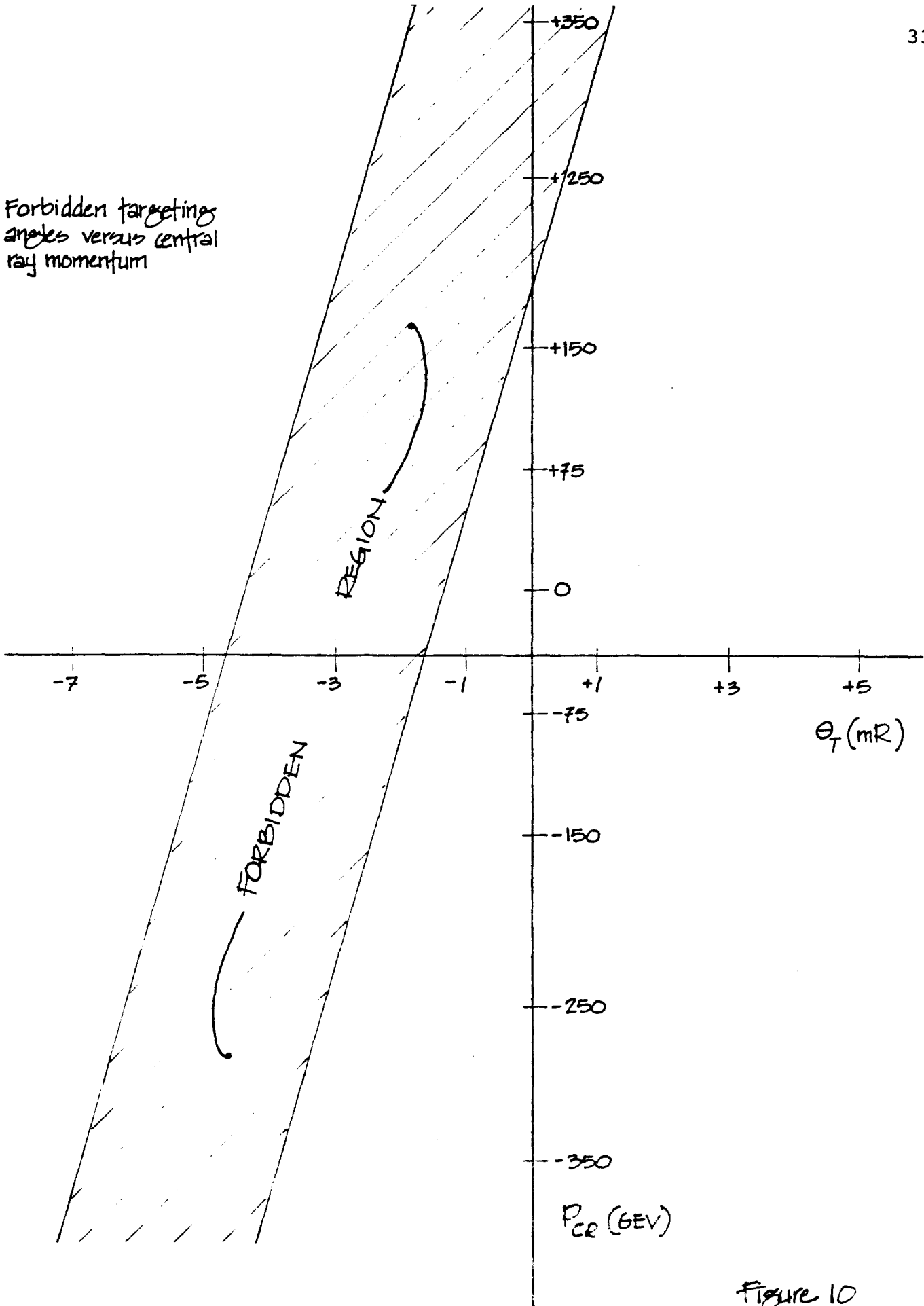


Figure 10

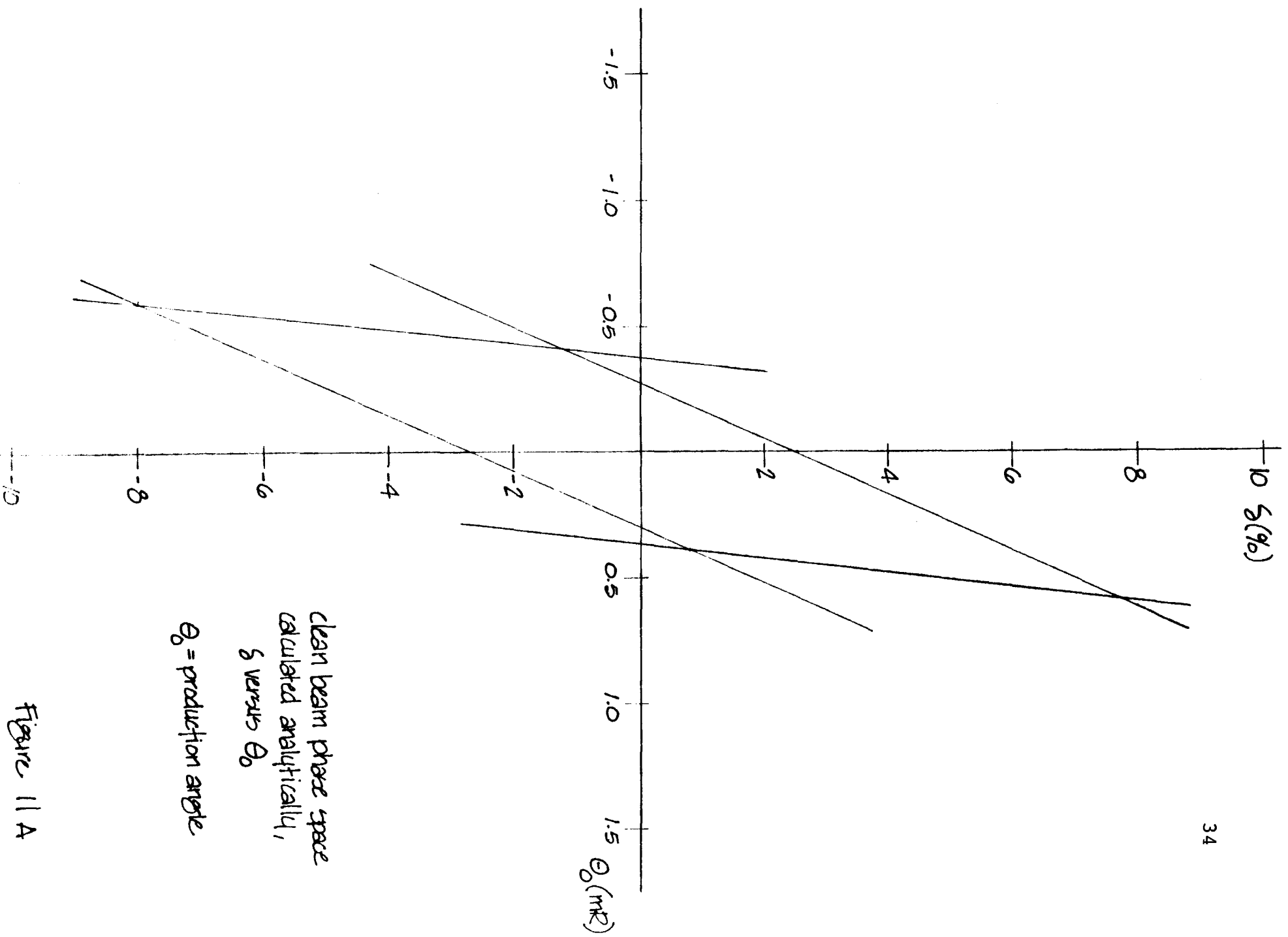


Figure 11A

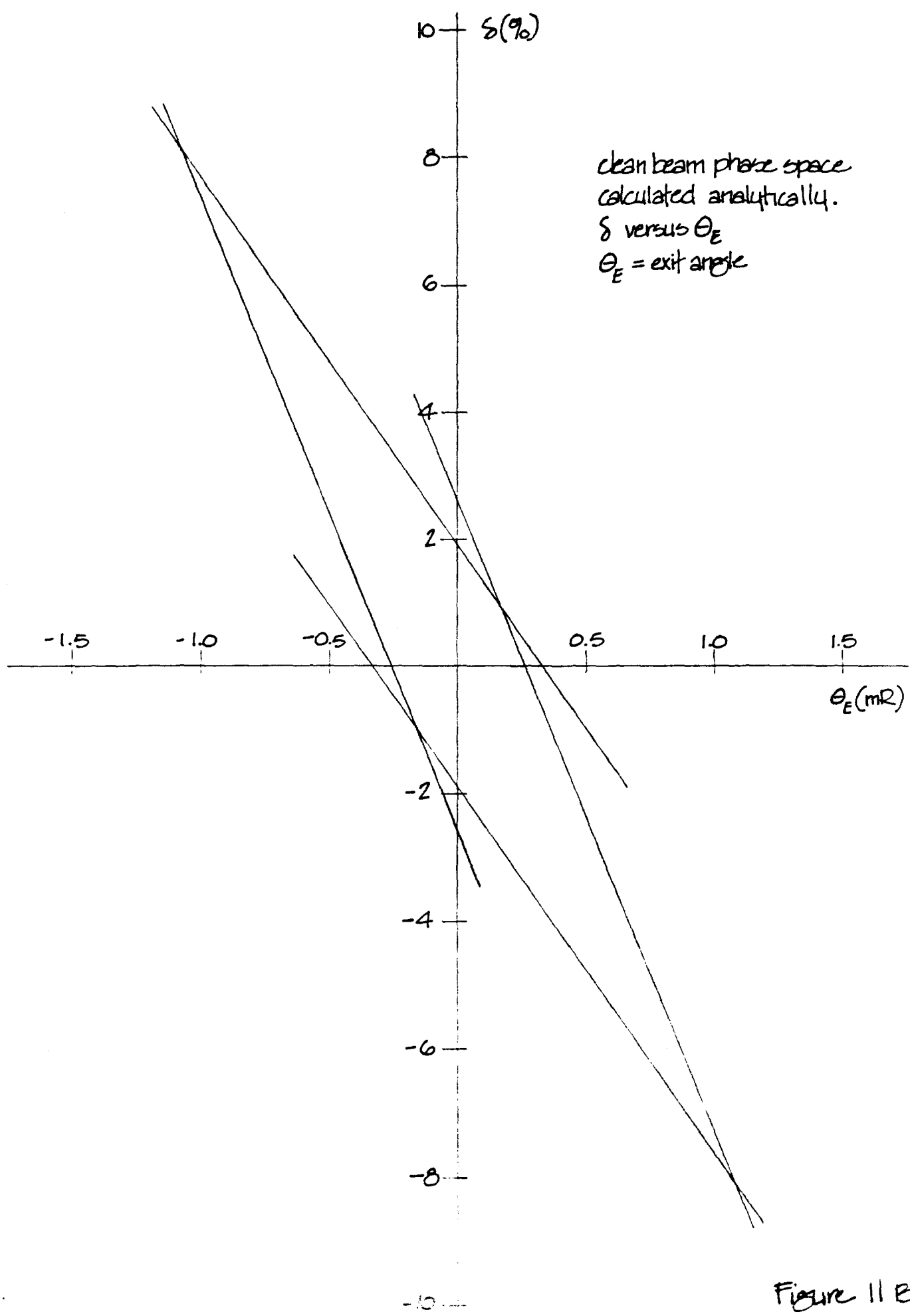
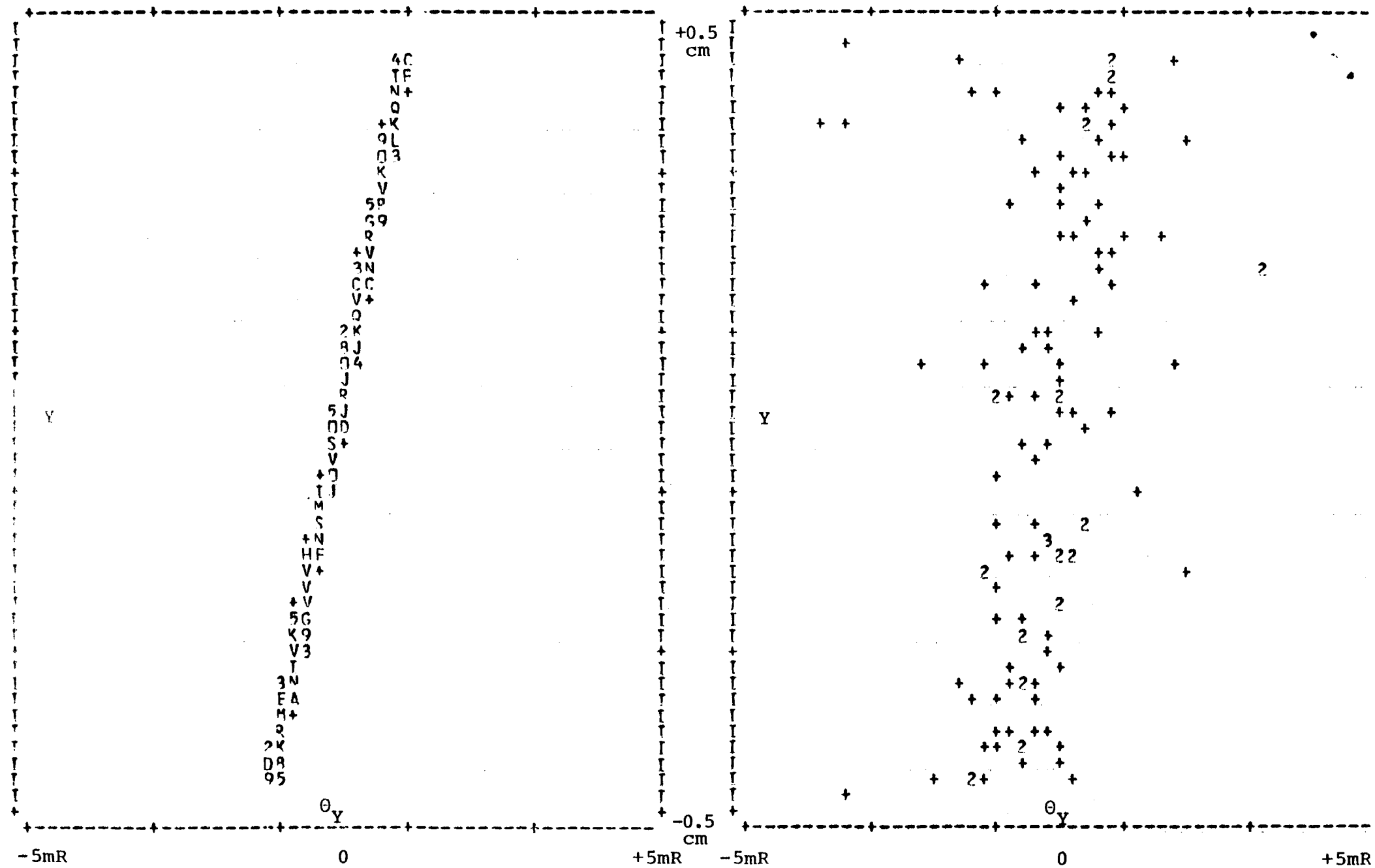


Figure 11 B



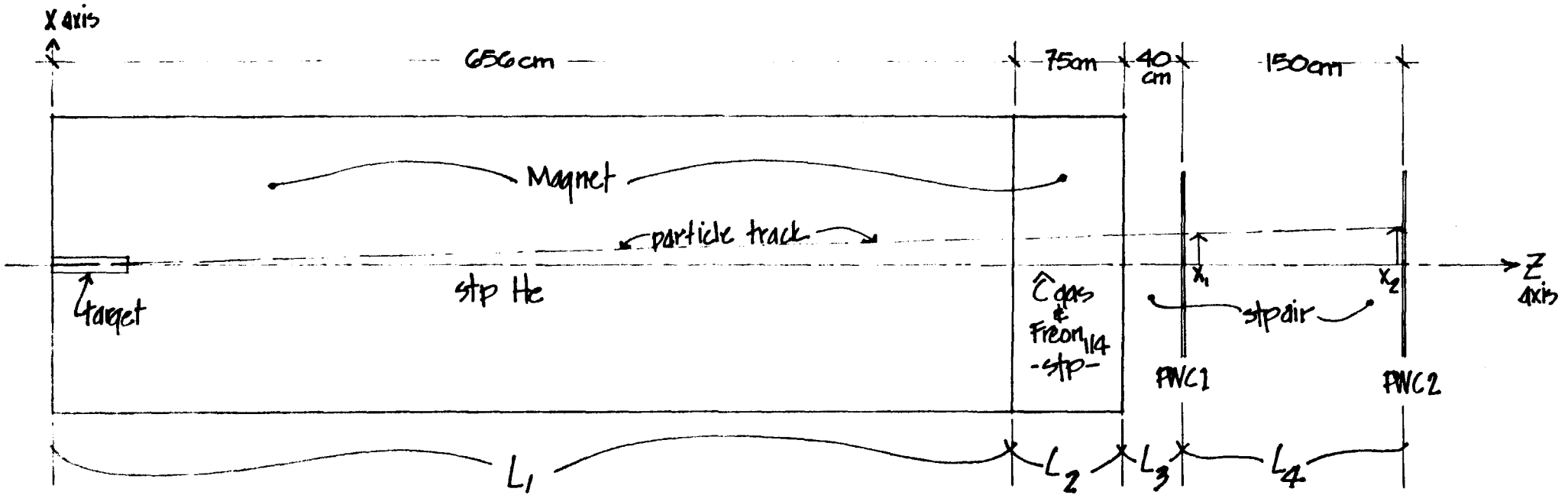
Clean Beam

Scattered Beam

Y versus θ_Y

38

Figure 11 E



we later define:

$$\hat{L} = L_1 + L_2$$

$$L = \hat{L} + L_3$$

Figure A.1